

## Etching a single micrometer-size particle in a plasma

W. W. Stoffels,\* E. Stoffels,\* G. H. P. M. Swinkels, M. Boufnichel,<sup>†</sup> and G. M. W. Kroesen  
*Eindhoven University of Technology, P.O. Box 513, 5600 MB Eindhoven, The Netherlands*

(Received 18 August 1998; revised manuscript received 26 October 1998)

Treatment of a single micrometer-size dust particle in a low-pressure radio-frequency discharge is presented. The particle is trapped in a potential well and its radius is accurately determined using angle-resolved Mie scattering. In an oxygen plasma, the particle radius can be decreased in a well-controlled way. [S1063-651X(99)13702-4]

PACS number(s): 52.25.Vy, 52.75.Rx, 42.68.Mj

In the past decade dusty plasmas have grown into an extensive research field. Numerous aspects of the formation, interactions and consequences of dust particles in plasmas have been investigated, ranging from dust dynamics in the interstellar space [1] to the dust contamination problem in industrial surface processing plasma reactors [2,3]. The new developments in dusty plasma science combine the knowledge from other research fields, such as dynamics of rarefied gases and aerosol physics, enriched with numerous electric interactions in the ionized medium.

The characteristic feature of an object immersed in the plasma is the negative electrical charge it acquires. In the steady state, the fluxes of positive ions and electrons from the plasma towards the solid surface must be equal. As electrons have a higher mobility than positive ions, an appropriate negative surface charge and electric field will be established to accelerate the positive ions and repel the electrons. Such effects occur for bounding surfaces, such as electrodes and plasma chamber walls, as well as for microscopic objects, such as dust particles. The potential difference between the particle and the plasma, the floating potential ( $V_p$ ), is a function of the electron temperature ( $T_e$ ). As in low-pressure discharges this potential is usually two to three times  $kT_e/e$ , for typical electron temperatures of approximately 3 eV, the floating potential is on the order of 10 V. The floating potential determines the energy of positive ions reaching the particle surface, as well as the number of elementary charges on the particle ( $Z$ ). The latter can be estimated from the classical expression  $Ze = 4\pi\epsilon_0 a V_p$ , where  $4\pi\epsilon_0 a$  denotes the capacitance of a sphere with a radius  $a$ . This simple expression for the particle charge yields approximately three elementary charges per nanometer radius of a particle:  $Z \approx 3 \times 10^9 a$ . A particle in the plasma is subject to various forces, the most important being the electrostatic, gravitation, neutral and ion drag, and thermophoretic forces. Coulomb repulsion between the negative charged particle and the electrodes in combination with the other forces allows us to obtain very stable, virtually motionless particle suspensions. Previous experiments have shown that one can easily control the particle position by influencing the force balance. Thus, the Coulomb

and ion drag forces are tuned by varying parameters such as plasma power and pressure [4] or changing the electrode geometry [5,6], thermophoresis is induced by temperature gradients [7], and gas dynamical forces are determined by the gas flow pattern [8].

Previous studies were mainly concerned with particle clouds in discharges [9,10]. Particles were formed in the plasma and their physical and chemical properties were investigated. Particles produced and/or processed in the plasma can have interesting properties, such as photoluminescence [11] or a multilayer structure [12]. However, it is difficult to understand and control complex plasma processes in which large amounts of not-well-defined particles are involved. Alternatively, some investigators injected well-defined particles into the discharge in order to study plasma-particle interactions. Particle dynamics, force balance, and formation of Coulomb crystals were intensively studied [13–15].

In our experiment we combine these approaches. We introduce a single, well-defined particle into the plasma and pinpoint it in a specially constructed potential well. We demonstrate that we can accurately determine the particle properties and influence them in a controlled way by means of plasma processing. In particular, we employ angle-resolved Mie scattering to monitor the particle radius and we control the particle size by means of etching in a low-power radio-frequency oxygen discharge.

A schematic overview of the experiment is shown in Fig. 1. We use commercial melamine-formaldehyde particles with a diameter of approximately 12  $\mu\text{m}$  and a refractive index of 1.68. For the particle injection, we use a particle-filled sieve, which is mounted on a manipulator arm. The measurements are performed in a GEC reference cell: a parallel-plate capacitively coupled 13.56-MHz radio-frequency reactor [16]. An aluminium ring (diameter 2 cm, thickness 1.5 mm) is placed on the lower powered electrode in order to create a potential trap, so the particles shed from the sieve are immediately “caught” at the glow-sheath edge above the metal ring. In this way it is possible to prepare a Coulomb crystal, but also to “freeze” a single particle in a fixed position. Angle-resolved Mie scattering is applied to monitor the particle size and refractive index as a function of time during plasma processing. The light source is an argon ion laser, linearly polarized in the direction perpendicular to the detection plane (see Fig. 1). The scattered light is collected by an optical fibre, passed through an interference

\*Electronic address: [stoffels@discharge.phys.tue.nl](mailto:stoffels@discharge.phys.tue.nl)

<sup>†</sup>Present address: ESPEO Université d'Orleans, Boîte Postale 6744, 12 Rue de Blois, 45067 Orleans, France.

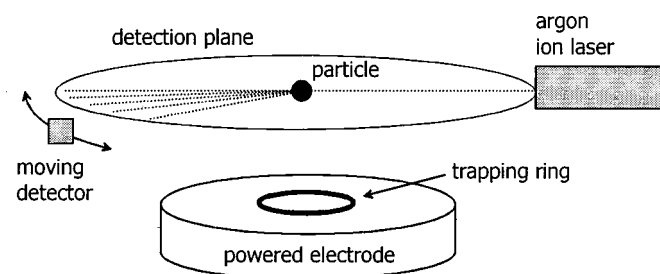


FIG. 1. Schematic view of the setup. A metal ring, placed on the electrode, creates a circular disturbance of the sheath above the ring. The potential well created in this way is used to trap a single particle at the plasma sheath boundary. Mie scattering measurements are performed using argon ion laser light ( $\lambda = 488$  nm), polarized perpendicular to the detection plane. An optical fiber mounted on a movable stage collects the scattered intensity in the forward direction. This allows a continuous angle-resolved detection of the scattered light between  $1^\circ$  and  $15^\circ$  with an angular resolution of  $0.06^\circ$ .

filter and fed to a photomultiplier. The optical fibre is mounted on a moveable stage. This allows continuous scanning of the detection angle in the range of  $1$ – $15^\circ$  for forward scattering. The maximum detection angle is limited only by the geometry of the optical ports of the GEC reactor. The angular resolution depends on the entrance opening of the optical fibre and its distance to the particle. In our case the square opening is  $1$  mm<sup>2</sup> and the distance is  $90$  cm, which results in an angular resolution of  $0.06^\circ$ . The angle-resolved scattering intensities are fitted to a numerical model for Mie scattering using the particle radius and refractive index as tuning parameters. A typical angle-resolved measurement and its fit to the data are shown in Fig. 2. As can be seen, there is a good agreement between the measured data and the fit. The fitted particle radius ( $a = 5.90$   $\mu\text{m}$ ) and refractive index ( $n = 1.68$ ) agree with the size determination using scanning electron microscopy (SEM) pictures and the data provided by the particle manufacturer. The particle size can be determined with an accuracy better than  $1\%$  by the angle-resolved scattering technique.

In order to demonstrate a good control of the particle radius and the sensitivity of the diagnostics, we use a low-power discharge to etch the particle material in a controlled

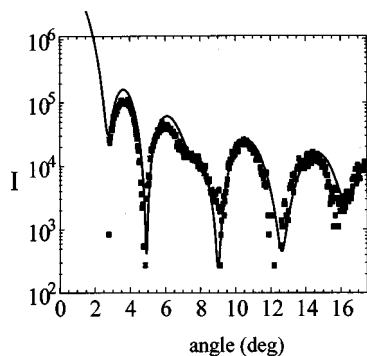


FIG. 2. Angle-resolved Mie scattering data of a single melamine-formaldehyde particle (squares), trapped in a radio-frequency oxygen plasma. The data are fitted by a theoretical scattering curve for a particle of a  $5.90$ - $\mu\text{m}$  radius and  $1.68$  refractive index.

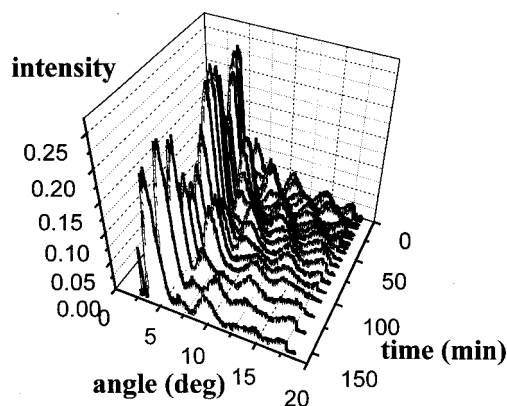


FIG. 3. Time-dependent angle-resolved scattering intensity of a single melamine-formaldehyde particle treated in a  $0.200$ -mbar,  $5$ -W oxygen plasma. The positions of the maxima and minima move to larger scattering angles with time, indicating that the particle size continuously decreases over time.

way. It should be noted that there is a large difference between the standard etching of a substrate placed on the electrode and the etching of a free floating particle in a plasma. In the sheath of the powered electrode a high potential on the order of  $1$  kV accelerates positive ions towards the surface. High-energy ions, reaching the electrode surface are responsible for sputtering and etching of the material. In contrast, the potential difference between the plasma and a floating particle is much lower, on the order of  $10$  V. Therefore, plasma chemical effects due to low-energy ions and radicals are expected to be most important for microscopic particle etching. In order to prove that there is no physical ion sputtering, we monitored time changes in the angle-resolved scattering signals of single particles trapped in argon and oxygen plasmas. In argon, where no chemical etching can occur, no remarkable changes were observed even after hours of plasma operation, while substantial variations of the scattering signal were recorded already after a few minutes of processing in oxygen. Oxygen is a well-known etching gas suitable for etching of organic polymer materials. Ion and radical chemistry in radio-frequency oxygen discharges was extensively studied in the past [17,18]. Free oxygen radicals and oxygen ions provide an ideal composition of active species to etch organic polymer particles trapped in the discharge.

Figure 3 shows the time evolution of the angle-resolved intensity scattered by a single particle in a  $5$ -W,  $0.2$ -mbar oxygen plasma. The characteristic Mie fringes are clearly visible, and it is evident that the maxima shift towards higher angles as the etching proceeds. In terms of the Mie theory, this implies that the particle size decreases over time. Using the numerical model the time-dependent particle size is deduced, as shown in Fig. 4. The corresponding etch rate for a single particle is  $0.1$  nm/s.

The etching process is determined by various plasma parameters. Tuning of these parameters provides a means of obtaining a good control of the etch rate and consequently of the particle radius. For example, we have investigated the influence of the plasma power on the etching process. The densities of reactive species in the discharge increase nearly linearly with increasing power, and the same dependence is expected for the etch rate. The particle was injected into a

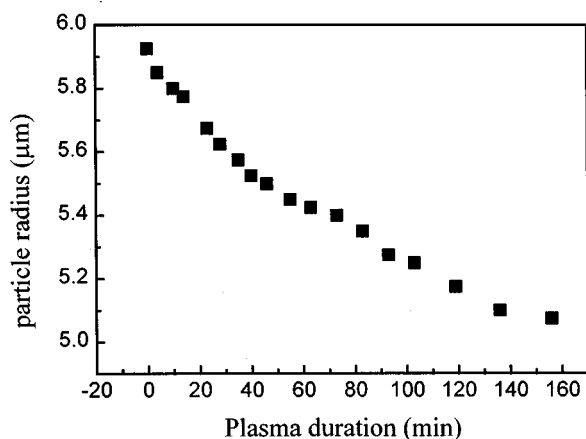


FIG. 4. Particle radius as a function of the treatment time in a radio-frequency oxygen plasma. The particle radius is determined by fitting the experimental data of Fig. 3 with theoretical Mie scattering intensities using the particle radius and refractive index as fitting parameters. Best fits are obtained by keeping the refractive index constant over time ( $n = 1.68$ ) and allowing the radius to decrease.

1.5-W oxygen discharge, and processed for about 30 min. At this power level only slight changes in the angle-resolved scattering intensity can be observed, which implies that the particle radius hardly changes (etch rate is 0.06 nm/s). After about 30 min the plasma power was increased to 5 W. At this power level etching of the particle proceeds faster (0.10 nm/s), which is reflected by time variations of the angle-resolved

scattering intensity. After 30 min of particle treatment in the 5 W plasma, the power was increased to 7 W. The plasma activity is further enhanced, resulting in an increased etch rate of 0.13 nm/s. Similarly, varying the pressure of the processing gas allows to etch the particles at a desired rate. By tuning of the plasma parameters, the etch rate can be varied from 0 up to 1 nm/s with an accuracy and reproducibility of approximately 10%. Similar etch rates were found for particle clouds [19].

We have shown that a single particle can be efficiently trapped in a discharge, and its size can be accurately regulated. We discuss etching as an example of such controlled particle treatment, but the presented technique opens many other possibilities. Particle size can be increased in deposition plasmas, e.g., using silane or methane [20]. Fine tuning of the particle size, at a well-defined rate, has undeniable benefits. For example, a particle modification process can be studied on a relatively simple, single-particle system, and extended to the situation of particle clouds. Moreover, the forces acting on a particle are size dependent, so an accurate determination and modification of particle size can prove extremely helpful in a study of the force balance and particle motion in the plasma.

This work was supported by the European Commission under Brite-Euram Contract No. BRPR CT97 0438 (HALU), by the Stichting voor Fundamenteel Onderzoek der Materie (FOM), and by the Dutch Technology Foundation (STW). The research of W.W.S. has been made possible by financial support from the Royal Netherlands Academy of Arts and Sciences (KNAW).

- 
- [1] *The Physics of Dusty Plasmas*, edited by P. K. Shukla (World Scientific, Singapore, 1996).
- [2] *Dusty Plasmas*, edited by A. Bouchoule (Wiley, New York, in press).
- [3] E. Stoffels, W. W. Stoffels, G. M. W. Kroesen, and F. J. De Hoog, *Electron Technol.* **31**, 255 (1998).
- [4] J. Kang, R. N. Carlile, J. F. O'Hanlon, and S. M. Collins, *J. Vac. Sci. Technol. A* **14**, 639 (1996).
- [5] R. N. Carlile, J. F. O'Hanlon, L. M. Hong, M. P. Garrity, and S. M. Collins, *Plasma Sources Sci. Technol.* **3**, 334 (1994).
- [6] G. S. Selwyn, *Plasma Sources Sci. Technol.* **3**, 340 (1994).
- [7] G. M. Jellum, J. E. Daugherty, and D. B. Graves, *J. Appl. Phys.* **69**, 6923 (1991).
- [8] W. W. Stoffels, E. Stoffels, G. M. W. Kroesen, and F. J. De Hoog, *J. Appl. Phys.* **78**, 4867 (1995).
- [9] H. M. Anderson and S. B. Radovanov, *J. Res. Natl. Inst. Stand. Technol.* **100**, 449 (1995).
- [10] J. B. Pieper, J. Goree, and R. A. Quinn, *J. Vac. Sci. Technol. A* **14**, 519 (1996).
- [11] C. Courteille, J.-L. Dorier, J. Dutta, Ch. Hollenstein, A. A. Howling, and T. Stoto, *J. Appl. Phys.* **78**, 61 (1995).
- [12] D. Vollath, D. Vinga Szabo, and J. Hausselt, *J. Eur. Ceram. Soc.* **17**, 1317 (1997).
- [13] D. A. Law, W. H. Steel, B. M. Annaratone, and J. E. Allen, *Phys. Rev. Lett.* **80**, 4189 (1998).
- [14] A. Homann, A. Melzer, S. Peters, and A. Piel, *Phys. Rev. E* **56**, 7138 (1997).
- [15] H. Thomas, G. E. Morfill, V. Demmel, J. Goree, B. Feuerbacher, and D. Moehlmann, *Phys. Rev. Lett.* **73**, 652 (1994).
- [16] P. J. Hargis, K. E. Greenberg, P. A. Miller, J. B. Gerardo, R. A. Gottscho, A. G. Bletzinger, J. R. Roberts, J. K. Olthoff, J. R. Whetstone, R. J. Van Brunt, H. M. Anderson, M. Splichal, J. L. Mock, M. L. Passow, M. L. Blake, M. E. E. Graves, D. B. Graves, M. J. Kushner, J. T. Verdeyen, G. Selwyn, M. Dalvie, J. W. Butterbaugh, H. H. Sawin, T. R. Turner, and R. Horwath, *Bull. Am. Phys. Soc.* **36**, 207 (1991).
- [17] E. Stoffels, W. W. Stoffels, D. Vender, M. Kando, G. M. W. Kroesen, and F. J. De Hoog, *Phys. Rev. E* **51**, 2425 (1995).
- [18] D. Vender, W. W. Stoffels, E. Stoffels, G. M. W. Kroesen, and F. J. De Hoog, *Phys. Rev. E* **51**, 2436 (1995).
- [19] G. H. P. M. Swinkels, E. Stoffels, W. W. Stoffels, N. Simons, G. M. W. Kroesen, and F. J. De Hoog, *Pure Appl. Chem.* **70**, 1151 (1998).
- [20] K. Tachibana, Y. Hayashi, T. Okuno, and T. Tatsuta, *Plasma Sources Sci. Technol.* **3**, 314 (1994).